ESRF	**Experiment title:** Time-resolved Bragg coherent X-ray diffraction imaging of the kinetics of physical processes in functional materials	**Experiment number**: MA-5129
Beamline: ID01	**Date of experiment**: from: 30 Jun 2022 to: 04 Jul 2022	**Date of report**: 26/09/2022
Shifts: 12	**Local contact(s)**: Edoardo Zatterin	*Received at ESRF:*

Names and affiliations of applicants (* indicates experimentalists):

T.W. Cornelius*, Aix-Marseille University, CNRS, IM2NP UMR 7334, Marseille, France

S. Matzen*, T. Maroutian*, A. Zing*, C2N, Université Paris-Saclay, CNRS, Palaiseau, France

Report:

This proposal aimed at studying the strain evolution in ferroelectric (FE) domains in ferroelectric $Pb(Zr,Ti)O_3$ (PZT) thin films by scanning X-ray diffraction microscopy (SXDM) during the application of an electric field. SXDM provides access to the strain with a resolution of 10^{-5} and lattice tilt with millidegree accuracy while the spatial resolution is defined by the beam size. The consecutive measurement after different voltage pulses allows for imaging the strain evolution and domain switching close to the coercive field.

Epitaxial ferroelectric PZT (Ti/Zr = 0.8) thin films with a thickness of ~150 nm were grown on $SrTiO_3$ by pulsed laser deposition, and integrated between top and bottom $SrRuO_3$ (SRO, conductive oxide) electrodes by classical optical lithography processes to define capacitors in order to apply *in situ* electric fields to modify and switch the FE domains. Fig. 1(a) shows the lithography mask used for the definiton of the top electrodes.

The incident X-ray beam at ID01 was monochromatized to 10 keV and focused to a size of 25 nm x 25 nm using a Fresnel zone plate with 300 µm in diameter and an outer zone width of 20 nm. Scanning X-ray diffraction images of two SRO top electrodes, of which the upper one is connected electrically to a Pt pad, is shown in Fig. 1(b) and (c) after the application of -2.2 V and +2.2 V, respectively. A slight intensity decrease is apparent for the upper SRO top electrode after the application of +2.2 V indicating the switching of ferroelectric domains. The domain switching induces a displacement of the ions in the unit cell which modify the structure factor and thus affect the diffraction intensity.

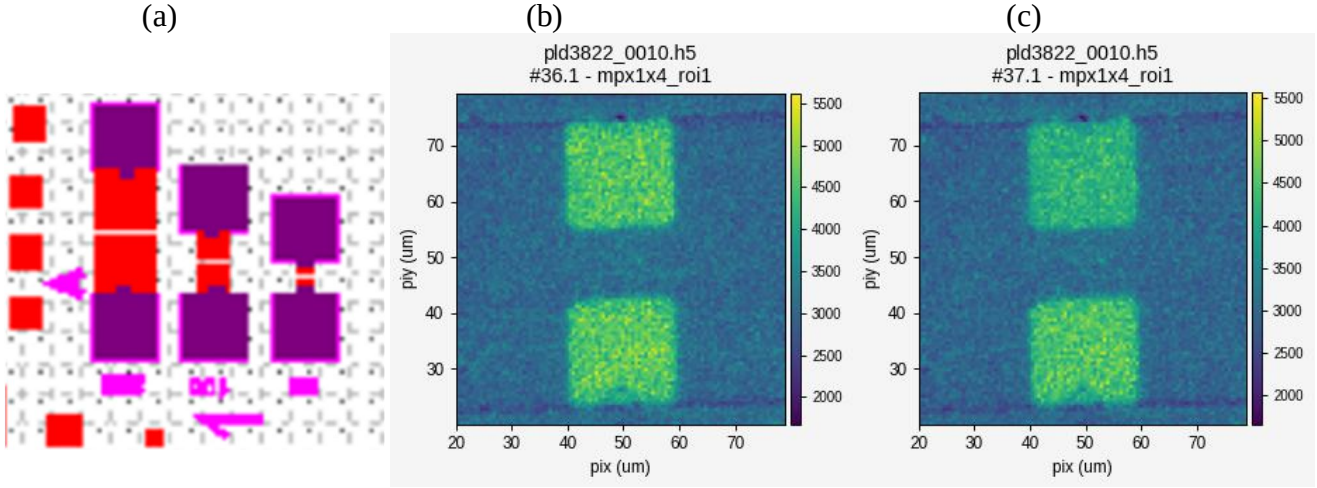

Fig. 1: (a) Part of lithography mask showing $SrRuO_3$ top electrodes (red) and Pt contact pads (purple). (b,c) SXDM images on neighboring $SrRuO_3$ electrodes, after (b) -2.2V and (c) +2.2V poling of the PZT under the top one.

We further measured SXDM on domains written py piezoresponse force microscopy (PFM). The PFM written domains are shown in Fig. 2(a) while a 2D SXDM map of the same area is presented in Fig. 2(b). The intensity variations clearly visualize the areas of domains with different orientations. 3D SXDM microscopy was recorded by mapping the same area for 20 different incident angles in the vicinity of the PZT 002 Bragg peak.

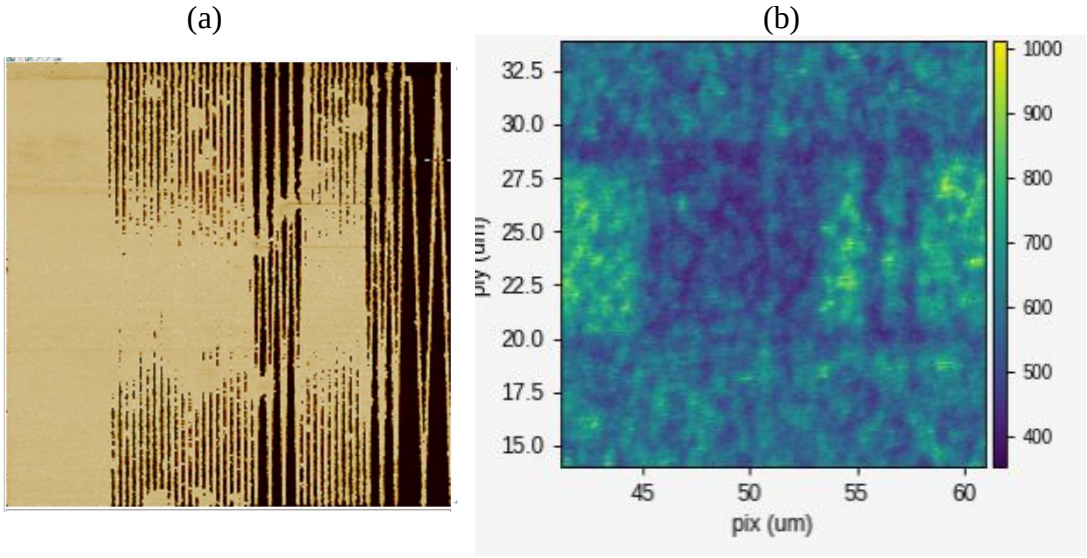

Fig. 2: (a) 10x10 μm^2 image of PFM phase showing written lines of down-oriented polarization (light areas) on up-oriented PZT film (dark areas).(b) SXDM map centered on the PFM-written zone, showing clear contrast in the written area.

Additional measurements were made on a different sample, a 100 nm-thick antiferroelectric $PbZrO_3$ (PZO) thin film that was prepared by pulsed laser deposition on a $SrTiO_3$ substrate and integrated between bottom SRO and top Pt electrode. The application of an electric field induces the transition of the PZO from antiferroelectric to ferroelectric state. This is accompanied by a change from an orthorhombic structure to a tetragonal structure. Theta-2 theta scans using a 1 µm X-ray beam were performed on PZO below Pt top electrode revealing the shift of the Bragg peaks of the antiferroelectric phase and the appearance of the Bragg peaks of the ferroelecrtic phase as a function of the applied voltage (Fig. 3).

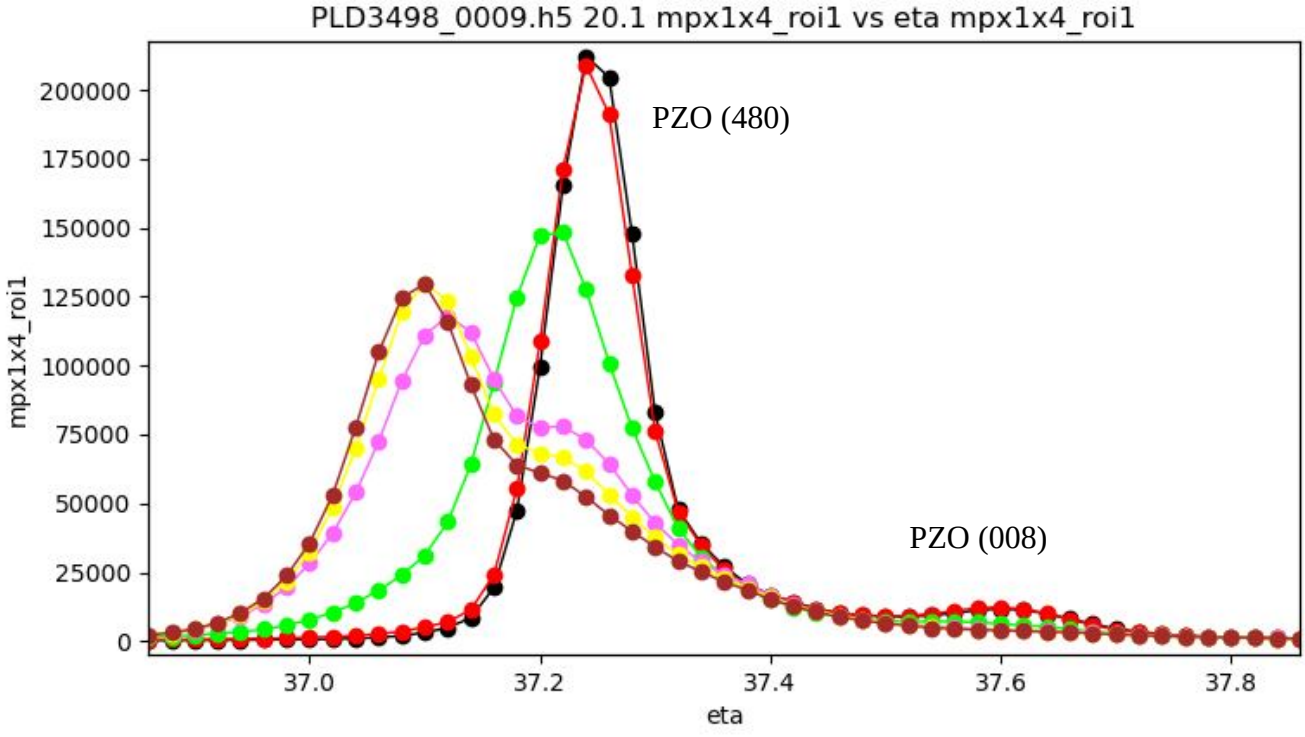

Fig. 3: (a) Theta-2Theta scans at 1 µm X-ray spot size around the (480) and (008) PZO diffraction peaks, showing their evolution with applied voltage and the appearance of a peak of the ferroelectric phase.

Moreover, SXDM with a 25 nm X-ray beam was performed during the application of a voltage mapping an area of 2 x 2 µm² with a step size of the X-ray probe. The antiferroelectric/ferroelectric phase transition is clearly visible in the SXDM images recorded at 0V , 1.5 V, and 2.5 V (Fig. 4). The phase transition does not evolve homogeneously underneath the Pt electrode: Circular areas are clearly apparent indicating nucleation centers of the phase transition from which the transition front propagates radially.

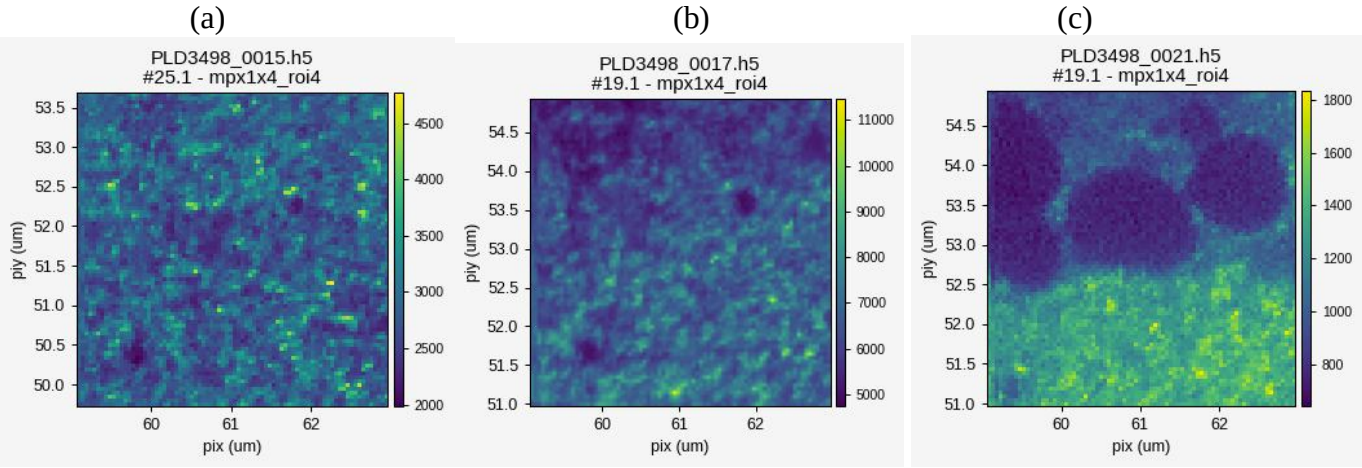

Fig. 4: (a) SXDM images at 25 nm X-Ray beam size showing the appearance of ferroelectric domains into the antiferroelectric PZO during application of (a) 0V, (b)+1.5V, and (c)+2.5V at the top electrode. The bottom part of the image is not below the Pt electrode thus not affected by electric field.

In summary, we demonstrated successful *operando* SXDM on ferroelectric PZT and antiferroelectric PZO thin films integrated in capacitor geometry. These experiments pave the way for future studies on ferroelectric domain structure in ferroelectric thin films and on the electrically driven antiferroelectric/ferroelectric phase transition using nanofocused X-ray beams.